

## Reductive activation of ricin and ricin A-chain immunotoxins by protein disulfide isomerase and thioredoxin reductase

Giuseppe Bellisola<sup>a</sup>, Giulio Fracasso<sup>a</sup>, Rodolfo Ippoliti<sup>b</sup>, Gianfranco Menestrina<sup>c</sup>,  
Anders Rosén<sup>d</sup>, Silvia Soldà<sup>a</sup>, Silvia Udali<sup>a</sup>, Rossella Tomazzolli<sup>c</sup>,  
Giuseppe Tridente<sup>a</sup>, Marco Colombatti<sup>a,\*</sup>

<sup>a</sup>Department of Pathology, Section of Immunology, University of Verona, Policlinico G.B. Rossi, L.go L.A. Scuro 10, I-37134 Verona, Italy

<sup>b</sup>Department of Pure and Applied Biology, University of L'Aquila, Via Vetoio, Coppito, I-67010 L'Aquila, Italy

<sup>c</sup>CNR-ITC, Section of Trento, Institute of Biophysics, Via Sommarive 18, I-38050 POVO (Trento), Italy

<sup>d</sup>Division of Cell Biology, Department of Biomedicine and Surgery, Linköping University, SE-581 85 Linköping, Sweden

Received 3 October 2003; accepted 13 January 2004

### Abstract

Intracellular activation of ricin and of the ricin A-chain (RTA) immunotoxins requires reduction of their intersubunit disulfide(s). This crucial event is likely to be catalyzed by disulfide oxidoreductases and precedes dislocation of the toxic subunit to the cytosol. We investigated the role of protein disulfide isomerase (EC 5.3.4.1, PDI), thioredoxin (Trx), and thioredoxin reductase (EC 1.8.1.9, TrxR) in the reduction of ricin and of a ricin A-chain immunotoxin by combining enzymatic assays, SDS–PAGE separation and immunoblotting. We found that, whereas PDI, Trx, and TrxR used separately were unable to directly reduce ricin and the immunotoxin, PDI and Trx in the presence of TrxR and NADPH could reduce both ricin and immunotoxin *in vitro*. PDI functioned only after pre-incubation with TrxR and the reductive activation of ricin was more efficient in the presence of glutathione. Similar results were obtained with microsomal membranes or crude cell extracts. Pre-incubation with the gold(I) compound auranofin, which irreversibly inactivates TrxR, resulted in a dose-dependent inhibition of ricin and immunotoxin reduction. Reductive activation of ricin and immunotoxin decreased or was abolished in microsomes depleted of TrxR and in cell extracts depleted of both PDI and Trx. Pre-incubation of U-937, Molt-3, Jurkat, and DU145 cells with auranofin significantly decreased ricin cytotoxicity with respect to mock-treated controls ( $P < 0.05$ ). Conversely, auranofin failed to protect cells from the toxicity of pre-reduced ricin which does not require intracellular reduction of disulfide between the two ricin subunits. We conclude that TrxR, by activating disulfide reductase activity of PDI, can ultimately lead to reduction/activation of ricin and immunotoxin in the cell.

© 2004 Elsevier Inc. All rights reserved.

**Keywords:** Ricin; Immunotoxin; Disulfide reduction; Protein disulfide isomerase; Thioredoxin; Thioredoxin reductase

### 1. Introduction

Many bacterial and plant toxins are composed of a toxic enzymatic subunit A covalently linked by a disulfide bond to the binding subunit B. This group of A–B toxins includes bacterial toxins such as shigella toxin [1], diphtheria toxin (DT) [2], pseudomonas exotoxin A (PEA) [3], cholera toxin (CT) [4], as well as the plant toxin ricin [5]. Ricin A-chain (RTA), the catalytic subunit of ricin, can be chemically cross-linked with a disulfide bridge to vehicle molecules (i.e. antibody or antibody fragments, growth factors, cytokines) to obtain immunotoxins (ITs) [6]. There is increasing interest in the medical applications of ITs, which have been successfully applied in several human diseases [7].

**Abbreviations:** Auranofin, *S*-triethylphosphine gold(I)-2,3,4,6-tetra-*O*-acetyl-1-thio- $\beta$ -D-glucopyranoside;  $\beta$ -MET,  $\beta$ -mercaptoethanol; CT, cholera toxin; DT, diphtheria toxin; DTT, dithiothreitol; ECL, enhanced chemiluminescence; ER, endoplasmic reticulum; GSH, reduced glutathione; GSSG, oxidized glutathione; HRP, horse-radish peroxidase; IT(s), immunotoxin(s); PBS, phosphate-buffered saline; PDI, EC 5.3.4.1, protein disulfide isomerase; bPDI, bovine liver PDI; RIPs, ribosome inactivating proteins; r.t., room temperature; RTA, ricin A-chain; RTA-ITs, ricin A-chain conjugated with a carrier antibody; RTB, ricin B-chain; ST.1-RTA, mouse anti-CD5 ST.1F(ab')<sub>2</sub> fragment conjugated with RTA; Trx, thioredoxin; hrTrx, human recombinant Trx (mutant C61S/C72S); TrxR, EC 1.8.1.9, mammalian thioredoxin reductase

\* Corresponding author. Tel.: +39-045-807-4256;  
fax: +39-045-820-2459.

E-mail address: [marco.colombatti@univr.it](mailto:marco.colombatti@univr.it) (M. Colombatti).

A key event in the intracellular activation of ricin and RTA-conjugates is the reduction of the disulfide bond between RTB and RTA subunits of ricin or between RTA and its carrier molecule [8]. After endocytosis ricin travels backward along the secretory pathway to the Golgi apparatus and endoplasmic reticulum (ER) where RTA is dislocated across the ER membrane to the cytosol [9]. During its journey within the cell ricin becomes reductively activated, possibly in the ER or in earlier compartments. Although partly influenced by the carrier molecule, ligand-bound RTA is likely to follow a similar routing pathway within the cell and ultimately localize in the ER. Following cytosol entry RTA removes a specific adenine base from 28S rRNA and interferes with EF-2 binding resulting in protein synthesis inhibition and cell death [10]. Reduction and unfolding of CT by protein disulfide isomerase (PDI) [11] is a prerequisite for the dislocation of CTA1 subunit from the ER to the cytosol [12,13]. A similar mechanism has been hypothesized for ricin [14] and is likely to occur also in the case of RTA-ITs.

In eukaryotic cells, the ubiquitous thioredoxin system (thioredoxin + thioredoxin reductase) [15] and the glutaredoxin system (glutaredoxin + glutathione reductase) [16] catalyze fast and reversible thiol–disulfide exchanges between cysteines in their active site and cysteines of their disulfide substrates using NADPH and GSH as a source of reducing equivalents, respectively. Thioredoxin (Trx) mainly localizes in the plasma membrane [17], cytoplasm, and mitochondria [18], whereas glutaredoxin is found in the cytoplasm and the nucleus [19,20]. Several proteins sharing little sequence similarity but possessing a common active site have been characterized in the superfamily of thioredoxins [21]. Among them PDI is found in the plasma membrane, in secretory vesicles, in the Golgi apparatus and most abundantly in the ER lumen [22], where PDI is recycled via a retrograde mechanism from the *cis*-Golgi network by a mechanism common to several different proteins with a KDEL signal localization sequence [23].

Thioredoxin reductase (TrxR) is a FAD containing pyridine nucleotide-disulfide oxidoreductase composed of two identical 57-kDa subunits in which a C-terminal selenocysteine residue is essential for enzyme activity [24,25]. The best characterized function of TrxR is to catalyze the transfer of reducing equivalents from NADPH to its natural substrate oxidized Trx, thus maintaining its disulfide reductase activity in the cell. It has been demonstrated *in vitro* that also PDI can be a substrate of TrxR [26]. Although the mechanism required to maintain the redox status of PDI in the cell has not been identified yet, interest has been recently focused on Ero1p, an ER resident oxidoreductase [27,28], whereas TrxR has so far received little attention. TrxR is highly expressed in microsomes and in the Golgi apparatus [29] where it might play a role in reducing PDI as well as other proteins of the thioredoxin family [21]; moreover TrxR is also found in the plasma membrane [30]. TrxR has broad substrate specificity and is

able to reduce a number of substrates besides Trx [31]. Several stimuli regulate TrxR synthesis in normal and pathological instances, including oxidative stress and cytokines [32] and various alkylating agents, quinones, and gold-containing organic compounds can inactivate TrxR by irreversible modification of selenium in the selenocysteine residue [33].

In the present work, we have investigated the possible role of TrxR in the reductive activation of ricin and of a RTA-based IT by Trx and PDI. The role of TrxR might be crucial in the cell intoxication phenomena mediated by ricin and by RTA-containing heteroconjugates, inasmuch as TrxR could enable disulfide reductase activity of PDI also in the cell, possibly in the Golgi and in the ER, where ricin and probably also RTA-ITs may become reductively activated. We herein present evidence that indeed TrxR exerts a fundamental role in the reduction of disulfides of ricin and of RTA-ITs by acting as a reductase not only of Trx but also of PDI.

## 2. Materials and methods

### 2.1. Materials

All chemicals described were of reagent grade. NADPH (tetrasodium salt) and complete protease inhibitor complex tablets were from Roche; *S*-triethylphosphine gold(I)-2,3,4,6-tetra-*O*-acetyl-1-thio- $\beta$ -D-glucopyranoside (auranofin) was from ICN Biomedicals; DTT, glutathione (both reduced, GSH and oxidized form, GSSG) and bovine liver PDI (EC 5.3.4.1, bPDI) were from Sigma-Aldrich; recombinant human Trx, (mutant C61S/C72S, hrTrx), mammalian TrxR (E.C. 1.8.1.9, specific activity  $\geq 20$  U/mg) and antibody to human Trx (goat) were from IMCO; polyclonal antibody to PDI (rabbit) was from StressGen Biotechnologies; antibody to human placenta TrxR (mouse IgG1 clone 2, recognizing the cytosolic TrxR1) was obtained by A.R. as previously described [34]. Polyclonal anti-RTA antiserum was purified from the serum of a hyperimmunized rabbit by immunoaffinity chromatography. Canine pancreatic microsomal membranes were supplied from Promega in a buffer containing 2 mM DTT.

### 2.2. Ricin toxin, pre-reduced ricin, and anti-CD5 S.TIF(ab')<sub>2</sub>-RTA immunotoxin

Ricin (a 63-kDa protein toxin from castor bean of *Ricinus communis*) was purified according to Nicolson and Blaustein [35]. Pre-reduced ricin was obtained by incubating native ricin ( $10^{-5}$  M) in phosphate-buffered saline (PBS), pH 7.2, with 5%  $\beta$ -mercaptoethanol ( $\beta$ -MET) for 4 h and was then dialyzed overnight against degassed and nitrogen-purged PBS containing 5 mM DTT to facilitate the reassociation of RTA and RTB subunits by non-covalent forces [36]. Excess DTT was

removed by gel filtration using BioGel P-6 columns (BioRad) equilibrated in PBS. All procedures were carried out at 4 °C. Pre-reduced ricin ( $4 \times 10^{-7}$  M) was then immediately utilized in cytotoxicity assays. Anti-CD5 ST.1F(ab')<sub>2</sub>-RTA immunotoxin (henceforth designated ST.1-RTA for brevity) was kindly supplied by Dr. P. Casellas (Sanofi Recherches) and was obtained by conjugation of a F(ab')<sub>2</sub> fragment of a murine anti-CD5 IgG2a monoclonal antibody with an average of two RTA molecules using the heterobifunctional cross-linker *N*-succinimidyl-3-(2-pyridyldithio)propionate (SPDP, Pierce). The IT has an average molecular weight of 160 kDa [37]. The reduction of the disulfide bond in pre-reduced ricin, the stability of the inter-chain disulfide bond of ricin and of ST.1-RTA and its complete reduction by 2% β-mercaptoethanol (β-MET) were checked by SDS-PAGE and immunoblotting analyses.

### 2.3. Cell cultures

The following human cell lines were utilized: U-937 (histiocytic lymphoma), Molt-3 (lymphoblastic leukemia), Jurkat (acute T cell leukemia), and DU145 (prostate carcinoma). All cell lines were purchased from the American Type Culture Collection and were maintained at 37 °C in a humidified atmosphere of 5% CO<sub>2</sub> by serial passages in RPMI 1640 additioned with 2 mM glutamine, 10% fetal bovine serum (FBS) and 50 U/ml of both penicillin and streptomycin. Cell lines were checked for mycoplasma contamination before use.

### 2.4. Spectrophotometric assay

To explore the ability of the Trx system (i.e. Trx + TrxR) and of the PDI system (PDI + TrxR) to reduce disulfide bonds of ricin and of ST.1-RTA, the procedure described by Magnusson et al. [38] was applied. The final reaction volume in the quartz cuvette was 300 μl. In brief, 400 μM NADPH, mammalian TrxR (45–90 nM, corresponding to 100–200 mU in the cuvette) and hrTrx (0.6–3.0 μM) or bIPDI (1–8 μM) were added to the assay buffer (100 mM potassium phosphate buffer, 2 mM EDTA, pH 7.4, KPE). After 5–10 min incubation at room temperature (r.t.), the reaction was initiated by adding ricin (1–2 μM) and NADPH consumption was monitored at 340 nm and at 25 °C. With an extinction coefficient  $E = 6200 \text{ M}^{-1} \text{ cm}^{-1}$  for NADPH the reduction of 1 μM disulfide corresponds to a  $\Delta A_{340 \text{ nm}}$  of 0.0062.

### 2.5. Gel electrophoresis and immunoblotting

The disulfide reductase activity of Trx and PDI on ricin and ST.1-RTA was studied by examining RTA separation from RTB (ricin) or from the antibody moiety (ST.1-RTA) on slab gels, followed by identification of fragments by immunoblotting with specific anti-RTA rabbit antibody.

Reactions were carried out in 1.5 ml Eppendorf polypropylene tubes containing the considered system (Trx + TrxR or PDI + TrxR) in a final volume of 50–100 μl reaction buffer (i.e. KPE buffer, NADPH to 200 μM, hrTrx to 1–3 μM or bIPDI to 1–8 μM and 90 nM mammalian TrxR corresponding to 35–70 mU). Tubes protected from light were incubated at r.t. for 20 min. After the reaction was initiated by addition of ricin or ST.1-RTA, samples were maintained at 37 °C and aliquots were collected at different times. In control tubes the same quantity of ricin or ST.1-RTA was added to the assay mixture in the absence of enzymes. A further control consisted of ricin or ST.1-RTA incubated with 2% β-MET in KPE and NADPH to completely reduce disulfide bonds of toxin and IT. The reaction was terminated by adding 10–20 μl of SDS/PAGE sample buffer with no reducing agents. Proteins were separated on a 10% slab gel (1 mm thickness) and transferred to a nitrocellulose membrane for immunoblotting. RTA was detected with polyclonal rabbit anti-RTA (1:500 v/v in TBST–0.2%BSA, overnight incubation at 4 °C) followed by HRP-conjugated anti-rabbit secondary antibody (1:1000 v/v in TBST–0.2%BSA solution for 2 h at 25 °C). Enhanced chemiluminescence (ECL, Pharmacia) detection procedure was applied. In experiments with ST.1-RTA, the membranes were re-blotted with HRP-conjugated polyclonal rabbit anti-mouse IgG (1:1000 v/v in TBST–0.2%BSA solution). Parallel experiments were carried out with canine microsomal membranes and with cell extracts (see below). After the first blotting with anti-RTA the membrane was re-blotted with anti-Trx or anti-PDI and developed in ECL with commercial HRP-conjugated mouse anti-goat Ig or HRP-conjugated mouse anti-rabbit Ig as secondary antibodies, respectively. To inhibit TrxR activity, dilutions of auranofin (50 nM to 10 mM) were prepared from a 100 mM stock solution in dimethyl sulfoxide (Sigma) immediately prior to use. After the first 20 min incubation, auranofin was added to the reaction mixture and tubes were further incubated for 20 min at r.t. and in the dark before initiating the reaction with ricin or ST.1-RTA. Samples and controls were analyzed by immunoblotting as described above.

### 2.6. Dithiol versus TrxR activation of PDI

We compared the ability of PDI, DTT-activated PDI, and TrxR-activated PDI to catalyze the reductive cleavage of RTA from RTB. DTT-activated PDI was prepared by incubating PDI with 10 mM DTT overnight at 4 °C and excess DTT was then removed by gel filtration using BioGel P-6 columns equilibrated in PBS, pH 7.4. To activate PDI by TrxR both enzymes were pre-incubated for 20 min at r.t. in KPE buffer containing 200 μM NADPH. The role of glutathione redox buffer was investigated by adding 750 μM GSH:250 μM GSSG or 750 μM GSSG:250 μM GSH, respectively, to KPE buffer containing 200 μM NADPH. Ricin was added to each system

containing GSH/GSSG at a 3:1 or 1:3 ratio. After incubation at 37 °C, the reaction was terminated by adding SDS/PAGE sample buffer and samples were analyzed by gel electrophoresis on a 10% slab gel.

### 2.7. Preparation of cell extracts

Cells (approximately  $6 \times 10^7$  to  $8 \times 10^7$  cells) washed three times with cold PBS were pelleted, resuspended in 1% NP-40 lysis buffer (50 mM Tris-HCl, pH 7.4 containing 150 mM NaCl and additioned with 0.1% complete protease inhibitors) and incubated 30 min in ice. The pellet was discarded and protein concentration in the supernatant was measured by the BCA method (Pierce) and adjusted to 4 mg/ml with lysis buffer. All procedures were carried out at 4 °C. Trx, TrxR, and PDI proteins in different cell extracts were separated on 10% slab gels and analyzed by immunoblotting using goat anti-human Trx, mouse anti-human TrxR, and rabbit anti-PDI antiserum, respectively.

### 2.8. Preparation of canine microsomal membranes

Pancreatic canine microsomal membranes were diluted in an equal volume of NP-40 lysis buffer (150 mM NaCl, 10% NP-40, 50 mM Tris-HCl pH 7.6) containing 0.1% complete protease inhibitors and incubated for 30 min in ice. After centrifugation at  $2000 \times g$  for 5 min, the supernatant was harvested, total protein content was measured by the BCA method and adjusted to 4 mg/ml.

### 2.9. Immunosubtraction experiments

Cell extracts and canine solubilized microsomal membranes were deprived of each system component (Trx, PDI, and TrxR, respectively) by immunoprecipitation with specific monoclonal or polyclonal antibodies and Protein-A-Sepharose. The efficiency of immunoprecipitation procedures was checked by immunoblotting of the subtracted component. Reductive cleavage of ricin in untreated and in depleted cell extract samples was performed in separate tubes in the presence of 400  $\mu$ M NADPH, 750  $\mu$ M GSH and 250  $\mu$ M GSSG. Control samples consisted of deprived cell extracts additioned with the immunosubtracted component.

### 2.10. Inhibition of ricin, pre-reduced ricin, and ST.1-RTA cytotoxicity by auranofin

$^{14}$ C-Leucine incorporation was measured to compare inhibition of protein synthesis by ricin in cells pre-incubated without or with the gold(I) compound auranofin. U-937, Molt-3, Jurkat, and DU 145 cells were resuspended in RPMI 1640 without leucine, with 2 mM glutamine and 5% FBS and plated in 96 microtiter flat-bottomed well plates ( $5 \times 10^4$  cells in a final volume of 80  $\mu$ l per well). Auranofin was diluted in RPMI 1640 w/o leucine and 10  $\mu$ l

of auranofin dilutions (3, 15, 30, 150, and 300 nM) were added in triplicate to sample wells. An equal volume of culture medium was added to control wells. Cells were then incubated at 37 °C in a humidified atmosphere of 5% CO<sub>2</sub> for different times. Ricin dilutions were prepared in RPMI 1640 w/o leucine from a stock of 1  $\mu$ M ricin solution in PBS. A 10  $\mu$ l volume of each ricin dilution (10 fM to 1 nM ricin) was added to samples 6 h before the end of the assay. Controls received an equal volume of culture medium. Four hours before the end of the assay a 10  $\mu$ l volume of  $^{14}$ C-leucine ( $3.7 \times 10^4$  Bq) was added to samples and controls. Cells were harvested and  $^{14}$ C-leucine radioactivity was measured in a beta spectrometer. Percent of  $^{14}$ C-leucine incorporation was plotted versus ricin and auranofin concentrations. We verified if auranofin could block other steps in ricin entry pathway by comparing the toxicity of ricin and pre-reduced ricin in four cell lines. Untreated cells or cells pre-incubated for 6 h with 30 nM gold(I) compound auranofin were exposed for 90 min to high concentrations ( $4 \times 10^{-7}$  M) of ricin or of pre-reduced ricin in the presence of  $^{14}$ C-leucine.

### 2.11. Statistics

Mean and error values of at least three separate experiments were calculated. Treatment differences were compared in each cell line and for each ricin concentration by Wilcoxon signed rank test or by paired *t*-test; *P* < 0.05 indicates the probability level for null hypothesis (ineffective protection by auranofin).

## 3. Results

### 3.1. Trx and PDI reduce ricin and ST.1-RTA in the presence of TrxR and NADPH in vitro

Five disulfide bonds are present in the heterodimeric ricin molecule at equilibrium: four of them stabilize the folding of RTB subunit whereas the fifth disulfide bridge links the C-terminus of RTA to the N-terminus of RTB [5]. We estimated that more than 12 disulfide bonds are present in the ST.1-RTA molecule and at least two of them hold together the mouse anti CD5 F(ab')<sub>2</sub> and the RTA molecule. As illustrated in Fig. 1, rapid NADPH consumption is observed when ricin or ST.1-RTA are added to Trx or PDI in the presence of fixed amounts of TrxR. In contrast, no change of absorbance at 340 nm is observed after the addition of toxin or IT to TrxR in the absence of Trx or PDI, thus suggesting that TrxR itself cannot reduce disulfides of ricin or of ST.1-RTA molecules. Taking into account the amount of NADPH consumed to reduce oxidized Trx or oxidized PDI it can be concluded that almost complete disulfide reduction of ricin and of ST.1-RTA has taken place. However, PDI was less efficient than Trx in reducing ricin or IT disulfides. In fact, five- to six-fold

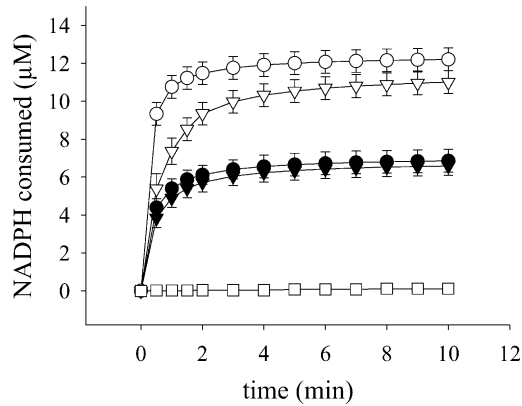


Fig. 1. Reduction of ricin (filled symbols) and ST.1F(ab')<sub>2</sub>-RTA (empty symbols) by 3 µM hrTrx + 90 nM TrxR system (circles) or by 8 µM bIPDI + 90 nM TrxR system (triangles) or by 90 nM TrxR (squares). The reaction (200 mU TrxR in a final volume of 300 µl) was carried out at 25 °C and initiated by the addition of 1.38 µM ricin or 1.0 µM ST.1F(ab')<sub>2</sub>-RTA. NADPH oxidation was followed for 20 min by monitoring the decrease of absorbance at 340 nm. Each point represents the average NADPH consumed (±S.E.M.) calculated in three separate experiments. In blank samples, an equal volume of buffer was added instead of toxin or IT and NADPH background consumption was subtracted. Solid lines represent non-linear regression through mean data values.

greater amounts of PDI are necessary to obtain reaction rates similar to those obtained in the presence of Trx.

Immunotoxin- or ricin-derived RTA stains as a double band of 30–33 kDa with anti-RTA antibody due to different glycosylation. Therefore, the appearance of a double band in this region indicates that reduction has occurred. Results of immunoblotting confirm that Trx and PDI exert disulfide reductase activity on both ricin and ST.1-RTA (Fig. 2) which in turn is dependent on the presence of TrxR. In fact,

the reductive separation of ricin to RTA + RTB catalyzed by Trx (Fig. 2A, left panel) or by PDI (Fig. 2B, left panel) are both inhibited by pre-incubation with auranofin (Fig. 2A and B, right panels). Maximal inhibition of 90 nM TrxR was observed at 100–500 nM auranofin, which is in agreement with a  $K_i$  value of 4.0 nM gold(I) compound auranofin, a selective TrxR inhibitor [39]. It should be noticed that incubation with the Trx or the PDI systems does not completely reduce ricin to RTA + RTB, as observed instead in control ricin samples which are completely reduced by 2% β-MET. However, it must be considered that both PDI and to a lesser extent Trx also catalyze reverse reactions in the presence of reductant(s), allowing disulfide bond formation in proteins [40]. The results of ST.1-RTA reductive cleavage by Trx and PDI systems are also shown in Fig. 2A and B (middle panels). We found that, as observed in the case of ricin (Fig. 2B, left panel), PDI at a concentration close to that of Trx is less efficient in catalyzing the reductive cleavage of RTA from ST.1-RTA (compare results of time-course shown in Fig. 2A and B, middle panels), which is in agreement with the slightly slower kinetics of PDI observed in the case of ST.1-RTA in the NADPH consumption assay (Fig. 1). In fact, no bands stain with anti-RTA antibody at the position expected for intact ITs in samples treated with Trx + TrxR (Fig. 2A, middle panel), thus suggesting that RTA has been efficiently cleaved from its carrier molecule. Instead, bands corresponding to intact ITs, although showing progressively lower intensity with time, never disappear in samples treated with PDI + TrxR (Fig. 2B, middle panel). A band of approximately 62 kDa stains with anti-RTA antibody in samples treated with Trx + TrxR (Fig. 2A, middle panel) but not in sam-

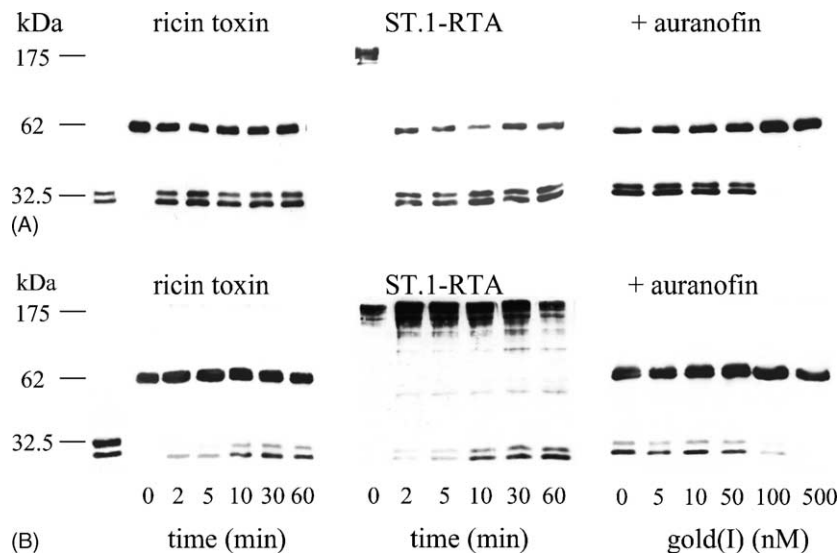


Fig. 2. Time-course of the NADPH-dependent reductive cleavage by 600 nM hTrx + 90 nM TrxR (A) or by 1.2 µM bIPDI + 90 nM TrxR (B), of 800 nM ricin (left panels) or ST.1-RTA (middle panels). Dose–response inhibition of ricin reduction by 20 min pre-incubation with the selective TrxR inhibitor gold(I) compound auranofin (right panels). The reaction mixture (50 µl) contained 35 mU TrxR. Nitrocellulose membranes were immunoblotted with rabbit polyclonal anti-RTA (no cross-reactivity with RTB) followed by HRP conjugated anti-rabbit secondary antibody and detected by ECL.

ples treated with PDI + TrxR (Fig. 2B, middle panel). This band may represent a heterodimer composed of an RTA molecule and a Fab fragment, as confirmed also by the appearance of a band migrating at the same position in samples stained with anti-mouse IgG antibody (not shown). Also in the case of ST.1-RTA auranofin completely inhibited reduction. Parallel results were obtained with other carrier molecule-toxin conjugates (not shown).

### 3.2. PDI activation and effects of redox buffer on the disulfide reductase activity of PDI

PDI appears to be a better thiol oxidant than disulfide reductant of proteins, particularly in the ER where the redox buffer equilibrium (dependent also on the GSH/GSSG ratio) is shifted towards a more oxidizing environment than in the cytosol [41]. Only in its reduced state PDI may intervene in the reduction of ricin. We, therefore, examined the role of reductants in the mechanism of action of PDI. As shown in Fig. 3, only PDI pre-activated with the reducing agent DTT (Fig. 3, lane 3) or PDI pre-incubated with TrxR (Fig. 3, lane 4) allow the NADPH dependent reductive separation of ricin subunits (approximately 2 and 10% yield of RTA, respectively, as opposed to 100% RTA yield in control ricin reduced with 2%  $\beta$ -MET; Fig. 3, lane 1), whereas untreated PDI does not lead to ricin subunits separation (Fig. 3, lane 2).

Disulfide reductase activity of PDI is more evident in the presence of 3:1 GSH:GSSG ratio (750  $\mu$ M GSH:250  $\mu$ M GSSG) redox buffer (approximately 25% RTA yield in DTT-PDI samples and approximately 50% RTA yield in TrxR-PDI treated samples; Fig. 3, lanes 5 and 6, respectively). Conversely, in the presence of a 1:3 GSH:GSSG ratio (250  $\mu$ M GSH:750  $\mu$ M GSSG), the disulfide reduc-

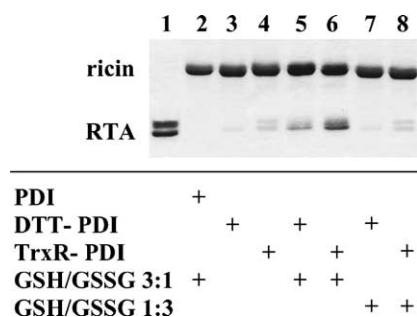


Fig. 3. Reduction of ricin by pre-reduced PDI. bPDI was pre-activated overnight by treatment with 200  $\mu$ M DTT (DTT-PDI), or by 20 min pre-incubation with 90 nM TrxR (TrxR-PDI) and NADPH. DTT was then removed by gel filtration. Some samples were added with 750  $\mu$ M GSH and 250  $\mu$ M GSSG (lanes 2, 5, and 6) or with 250  $\mu$ M GSH and 750  $\mu$ M GSSG (lanes 7 and 8). NADPH (200  $\mu$ M) was present in all samples. The reaction mixture (100  $\mu$ l) contained 70 mU TrxR. After 30 min incubation at r.t. to completely activate the system 800 nM ricin was added to all samples that were further incubated at 37 °C. Reaction was stopped after 60 min by addition of non-reducing sample buffer. Lane 1: ricin reduced with 2%  $\beta$ -MET; lane 2: bPDI; lanes 3, 5, and 7: DTT pre-activated PDI; lanes 4, 6, and 8: PDI pre-activated with TrxR.

tase activity of both DTT-PDI and TrxR-PDI is decreased, resulting in a RTA yield similar to that obtained in the presence of buffer without glutathione (Fig. 3, lanes 7 and 8, respectively). Therefore, although not strictly necessary, the presence of GSH in the reaction results in a more efficient ricin reduction by PDI pre-reduced with TrxR.

### 3.3. Reductive cleavage of ricin and of ST.1-RTA by microsomal membranes and cell extracts

Ricin has been localized in the ER lumen [9] where its reductive activation might take place due to the intervention of as yet unidentified disulfide reductase(s). Both TrxR and PDI are associated with the ER and could cooperate in the reductive activation of ricin and RTA-ITs. Therefore, we first investigated the expression of PDI and TrxR and the reductive cleavage of ricin in microsomal membranes (Fig. 4). Results of immunoblotting are summarized in Fig. 4A. PDI and TrxR were identified in microsomal membranes with a rabbit anti-PDI antiserum and with a mouse anti human TrxR monoclonal, respectively. Bands of lower molecular weight identified in samples immunoblotted with mouse anti human TrxR most likely represent breakdown products of TrxR [34]. Fig. 4B illustrates the time-course of ricin reduction obtained by incubating the toxin with canine microsomal membranes in KPE buffer containing NADPH and GSH:GSSG in a 3:1 ratio. Pre-incubation of microsomes with auranofin considerably suppressed the disulfide reductase activity at concentrations above 5–10 nM. Residual reduction of ricin observed in inhibition assays carried out in the presence of auranofin could be attributed to trace amounts of DTT present in canine microsomes and triggering disulfide reductase activity of PDI, as observed in other instances (see also

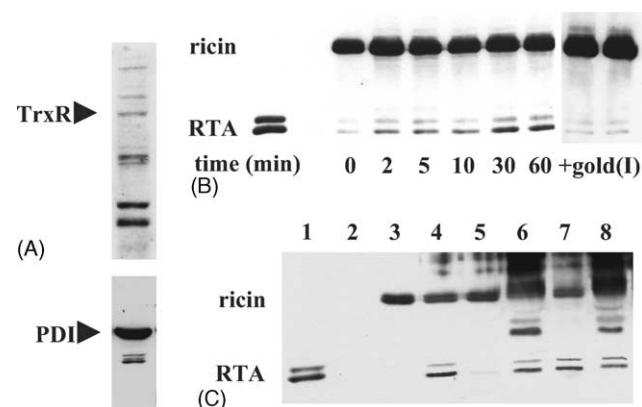


Fig. 4. (A) Identification of TrxR and PDI in pancreatic canine microsomal membranes by immunoblotting using anti human TrxR monoclonal antibody (upper panel) and rabbit anti PDI (lower panel). (B) Time-course of ricin (1.0  $\mu$ M) reduction by microsomal membranes and inhibition of TrxR by 20 min pre-incubation with 30 nM gold(I) compound auranofin. (C) Reduction of ricin by microsomal membranes immunosubtracted of TrxR (lane 5), PDI (lane 6), Trx (lane 7), or PDI and Trx (lane 8). Control samples included ricin reduced with 2%  $\beta$ -MET (lane 1), non-reduced ricin (lane 3); untreated intact microsomes (lane 4).

Fig. 3), or directly reducing disulfide bonds of ricin. Decreased or absent ricin chains separation was observed in microsomes immunodepleted of TrxR (Fig. 4C, lane 5). However, trace amounts of DTT which could not be eliminated from microsomes resulted in the appearance of minute amounts of RTA. Taken together, these results further support the hypothesis that TrxR associated with microsomes is necessary to sustain disulfide reductase activity of PDI.

Activation of both ricin and abrin toxins by cytosolic extracts was described by Barbieri et al. and attributed to a GSH-dependent 40 kDa protein disulfide reductase(s) [42]. In the attempt to positively identify cellular agents that could be crucially involved in the reductive activation of ricin, we first examined the expression levels of Trx, TrxR and PDI in different cell lines by immunoblotting of crude cell extracts. Crude untreated cell extracts were used to reduce ricin and results were compared with those obtained using cell extracts pre-incubated with auranofin or immunodepleted of Trx, TrxR, or PDI or combinations thereof to assess the role of the various enzymes. Fig. 5A shows the expression of Trx, TrxR, and PDI in crude U-937, Molt-3, Jurkat, and DU145 cell extracts. TrxR was found in similar amounts in extracts of all cell lines, whereas Trx and PDI showed higher levels of expression in the U-937 cell line.

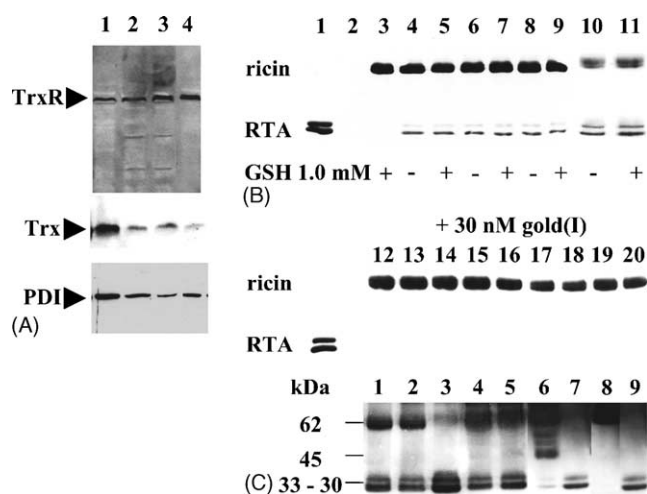


Fig. 5. (A) Immunoblot identification of TrxR, Trx, and PDI in cell extracts. Lane 1: U-937; lane 2: Molt-3; lane 3: Jurkat; lane 4: DU145. (B) Reduction of 1.0 μM ricin by cell extracts (30 μg total protein). Lane 1: control untreated RTA; lane 3: control untreated ricin; lanes 4 and 5: U-937 cell extracts; lanes 6 and 7: Molt-3 cell extracts; lanes 8 and 9: Jurkat cell extracts; lanes 10 and 11: DU145 cell extracts. Reduction of 1.0 μM ricin by cell extracts pre-incubated for 20 min with 30 nM gold(I) compound auranofin; lane 12: control untreated ricin; lanes 13 and 14: U-937 cell extracts; lanes 15 and 16: Molt-3 cell extracts; lanes 17 and 18: Jurkat cell extracts; lanes 19 and 20: DU145 cell extracts. (C) Reduction of 1 μM ricin by U-937 cell extracts (30 μg total protein) immunosubtracted of Trx (lane 2), PDI (lane 4), and TrxR (lane 6) or Trx and PDI (lane 8). Lane 1: control untreated U-937 cell extract; lane 2: cell extract w/o Trx; lane 3: cell extract w/o Trx + 1.0 μM hrTrx; lane 4: cell extract w/o PDI; lane 5: cell extract w/o PDI + 1.0 μM blPDI; lane 6: cell extract w/o TrxR; lane 7: cell extract w/o TrxR + 90 nM TrxR; lane 8: cell extract w/o Trx and PDI; lane 9: cell extract w/o Trx and PDI + 1.0 μM hrTrx and 1.0 μM blPDI.

The addition of 1 μM ricin to cell extracts (each 30 μg total protein) incubated in KPE and NADPH resulted in the reduction of ricin and the separation of RTA on a 10% slab gel irrespective of the presence or absence of 1.0 mM GSH in the reaction buffer (Fig. 5B). Moreover, pre-incubation of each cell extract with 30 nM gold(I) compound auranofin totally suppressed the reductive cleavage of ricin by cell extracts (Fig. 5B, lanes 12–20). As expected, immunosubtraction of Trx (Fig. 5C, lane 2) did not abolish the reductive cleavage of ricin in U-937 crude cell extract which is observed also when the U-937 cell extract is depleted of PDI instead of Trx (Fig. 5C, lane 4), thus suggesting that Trx and PDI may substitute each other as protein disulfide reductases in the cell. Moreover, TrxR subtraction (Fig. 5C, lane 6) did not completely abolish ricin reduction which was almost totally suppressed (>95%) in U-937 cell extract depleted of Trx and PDI (Fig. 5C, lane 8). In addition to RTA, immunoblotting revealed a further band in the 45 kDa region in TrxR immunodepleted sample (Fig. 5C, lane 6). This band (also observed in microsomal extracts and shown in Fig. 4C, lanes 6 and 8, respectively) is likely to represent complexes of RTA and unknown protein(s). This aspect warrants further investigation. Unlike what observed in microsomes absence of contaminating DTT in cell extracts failed to produce residual uncatalyzed ricin reduction.

#### 3.4. Inhibition of ricin and of pre-reduced ricin cytotoxicity by auranofin

Cleavage of disulfide bonds is a critical event in the activation of endocytosed toxins and ITs in the cell intoxication phenomena brought about by these molecules. In the case of ricin this step appears to be rate limiting [8] and may be linked to the process of translocon-assisted transmembrane passage [9]. Once in the cytosol RTA will inhibit protein synthesis thereby killing the cell. Because results of our in vitro experiments suggested that reductive activation of ricin cytotoxicity was crucially dependent on TrxR, we decided to evaluate the role of TrxR in intact cells by inhibiting its activity with auranofin. Thus, U-937, Molt-3, Jurkat, and DU145 cells were pre-incubated with auranofin to inhibit TrxR and ricin toxicity was evaluated in treated and untreated cells. As summarized in Fig. 6, the percentage of <sup>14</sup>C-leucine incorporation was significantly higher, and therefore ricin cytotoxicity lower, in cells incubated with 30 nM auranofin than in mock-treated control cells (Wilcoxon signed rank test:  $P < 0.05$ ). To rule out that auranofin could interfere with other steps of ricin-mediated intoxication, cells were also exposed in short-time assays to high doses of pre-reduced ricin (Fig. 7). Under these conditions, the reduction of the intersubunit disulfide is not rate limiting for ricin cytotoxicity [36]. As illustrated in Fig. 7, cytotoxicity of intact ricin was significantly decreased in cells pre-incubated with auranofin with respect to mock-treated controls

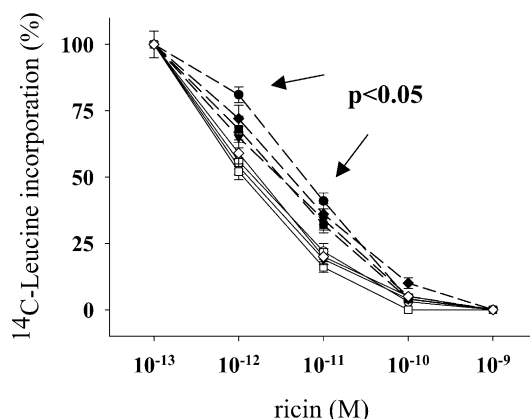


Fig. 6. Inhibition of ricin cytotoxicity by gold(I) compound auranofin. U-937 (circle), Molt-3 (triangle), Jurkat (square), and DU145 (diamonds) cells were pre-incubated in the absence (empty symbols) or in the presence of 30 nM auranofin for 6 h and were then exposed to ricin for 4 h. Protein synthesis was then measured by evaluating  $^{14}\text{C}$ -leucine incorporation. Results are expressed as percent  $^{14}\text{C}$ -leucine incorporation with respect to mock-treated control cultures. Each symbol represents mean values ( $\pm$ error) of three separate experiments. Arrows indicate ricin concentrations where significant differences between cells treated with or without auranofin were observed.

(*t*-paired test,  $P < 0.05$ ), whereas toxicity of pre-reduced ricin was not significantly different in cells pre-incubated with auranofin with respect to controls. Therefore, auranofin preferentially blocks toxicity of intact ricin but not that of pre-reduced ricin. Noteworthy, 30 nM gold(I) can totally inhibit reductive activation of ricin by microsomes (see above; Fig. 4), but ricin cytotoxicity can only be reduced and not abolished in cell lines under these conditions. This may suggest that additional mechanism(s) leads to ricin activation in intact cells.

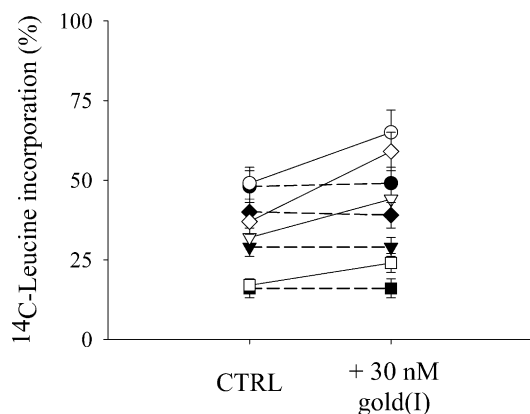


Fig. 7. Comparison of cytotoxic effect of intact ricin (empty symbols) and pre-reduced ricin (filled symbols) in U-937 (circle), Molt-3 (triangle), Jurkat (square), and DU145 (diamonds) cells in the absence or in the presence of 30 nM gold(I) compound auranofin. Cells were pre-incubated in the absence or in the presence of auranofin for 6 h and were then exposed to  $4 \times 10^{-7}$  M intact ricin or pre-reduced ricin for 90 min. Protein synthesis was then measured by evaluating  $^{14}\text{C}$ -leucine incorporation. Results are expressed as percent  $^{14}\text{C}$ -leucine incorporation with respect to mock-treated control cultures. Each symbol represents mean values ( $\pm$ error) of three separate experiments.

#### 4. Discussion

The reductive cleavage of disulfide bonds is an event of crucial importance to activate many bacterial and plant toxins in the cell. In particular, the reduction of the disulfide between RTA and RTB or a carrier molecule and the RTA subunit is necessary to activate RTA cytotoxicity of ricin and of RTA-ITs [9]. Indeed, the replacement of the intermolecular disulfide by a non-cleavable thioether linkage renders almost ineffective the toxicity of RTA-based ITs [43]. Reducing substrates such as GSH can facilitate thiol–disulfide exchange in the absence of enzymes but the presence of oxidoreductases increases the reaction rate by several thousand-fold [44]. The involvement of oxidoreductases is, therefore, likely to facilitate the intracellular activation of ricin and RTA-ITs and the subsequent cell intoxication phenomena.

Considering its intracellular localization, PDI appeared as the most likely candidate oxidoreductase to be involved in ricin and RTA-ITs reductive activation. The direction of the reaction catalyzed by protein disulfide oxidoreductases is determined by substrate and product concentrations, redox potential and the redox conditions of the cellular milieu. However, when PDI or Trx catalyze the reduction of disulfide bridges they become oxidized and therefore must be enzymatically regenerated by a reductase in order to maintain their catalytic activity as disulfide reductases. This is particularly true for PDI, which acts in the unfavorable redox oxidizing environment of the ER [41,45]. The selenoenzyme TrxR regenerates the redox status of Trx in intact cells and can also regenerate directly the cysteines in the active site of PDI in vitro or indirectly by means of Trx and NADPH [26]. Results of experiments reported herein indicated that neither ricin nor ST.1-RTA were directly reduced by TrxR. Therefore, in the most likely scenario PDI and TrxR would cooperate in ricin and RTA-ITs reduction intracellularly.

With our in vitro experiments, we first aimed at demonstrating that ricin and a RTA-IT (ST.1-RTA) could be reduced not only by the Trx system (i.e. Trx + TrxR), but also by the PDI system (i.e. PDI + TrxR). Our results clearly indicate that Trx and PDI can catalyze the reductive activation of both the toxin and the IT in a time-scale of seconds to minutes whereas the presence of TrxR appears to be essential to promote and sustain the disulfide reductase activity of the two oxidoreductases. Indeed, the reductive activation of ricin and of ST.1-RTA was dose-dependently inhibited by the gold(I) compound auranofin, an irreversible alkylating agent of selenium, which is necessary for the reductase activity of TrxR. To the best of our knowledge the demonstration that ricin and RTA-ITs could be reduced by PDI and TrxR has never been reported before.

The mechanism by which TrxR activates PDI and promotes its disulfide reductase activity in an oxidizing environment is suggested by results shown in Fig. 3. Unlike

PDI pre-incubated with the non-physiological reducing agent DTT, PDI pre-incubated with TrxR and NADPH allowed the reductive activation of ricin also in the absence of GSH, although a greater efficiency in ricin cleavage is shown by PDI when both TrxR and GSH/GSSG in a ratio of 3:1 are present together in the reaction buffer. Therefore, we hypothesized that reductive activation of ricin in microsomes could be ascribed to the reductase activity of TrxR on PDI. In fact, we found that both TrxR and PDI are expressed in microsomal membranes. Moreover, microsomal membranes incubated with NADPH and GSH/GSSG (3:1 ratio) allowed the time-dependent reduction of ricin and ST.1-RTA, which was in turn dose-dependently inhibited by pre-incubating microsomes with auranofin. In addition, results of immunosubtraction experiments confirmed that PDI and TrxR are indeed involved in the reduction of ricin in microsomes.

Immunosubtraction experiments carried out with cell extracts indicated that PDI can supply disulfide reductase activity on ricin also when Trx is absent. Consistent with the central role of TrxR in promoting the disulfide reductase activity of both Trx and PDI, incubation of cell extracts with auranofin inhibited the reductive cleavage of ricin (Fig. 5B) and of ST.1-RTA (not shown).

Similar ricin reduction patterns were observed in microsomes deprived of PDI (Fig. 4C, lane 6) or of PDI and Trx (Fig. 4C, lane 8) and in U-937 cell extracts deprived of TrxR (Fig. 5C, lane 6). In both cases, an effective reduction of ricin to RTA and RTB has occurred and a major band at approximately 45 kDa stained with anti-RTA antibody. To explain these apparently conflicting results it could be hypothesized that in microsomes other disulfide reductases (e.g. thioredoxin-related transmembrane protein, TMX, [21,46]) in addition to PDI or Trx (if present) may operate the reductive activation of ricin under the control of TrxR. Unlike microsomes, in cell extracts different cell compartments may merge. It can thus be speculated that in TrxR-depleted U-937 cell extract oxidized Trx and PDI could be directly reduced by high cytosolic GSH which may functionally replace TrxR [47]; alternatively reduction could be catalyzed or by other selenium-dependent TrxRs (e.g. mitochondrial TrxR) which were not recognized and immunosubtracted by the anti-TrxR antibody used by us. Inhibition of ricin reduction by non-immunodepleted U-937 cell extracts pre-incubated with auranofin (Fig. 5B, lanes 13 and 14) is in support of this second hypothesis. Therefore, the apparent discrepancy observed between data obtained with microsomes and with cell extracts can be attributed to different GSH content and/or may reflect the contribution of selenodependent reductase activity from different organelles present in the cell extract as a result of cell lysis. However reductive activation of ricin in intact cells is a strictly compartmentalized event and it might, therefore, take place in the ER or in ER-related organelles. It could be worthwhile also to identify which protein(s) or protein fragment(s) associates with RTA

resulting in a complex migrating at 45 kDa. Chaperones involved in RTA transport/unfolding process could be discovered.

Results of experiments conducted with intact cells confirmed our hypothesis that TrxR is central in the process of ricin/RTA-ITs reduction/activation. Similar TrxR expression was observed in U-937, Molt-3, Jurkat, and DU145 cell extracts whereas different expression levels of the PDI and Trx systems were observed. Nevertheless, comparable reductive cleavage of ricin was obtained in cell extracts from the four different cell lines. However, it must be considered that levels of protein expression and enzyme activity may not always correspond. Moreover, to explain the comparable reductive cleavage of ricin obtained in cell extracts from the four different cell lines we must also take into account that PDI can supply disulfide reductase activity on ricin also when Trx is absent.

The possibility that auranofin could block other crucial steps in the cell intoxication mechanism by ricin was ruled out by results obtained in control experiments with pre-reduced ricin. In fact, as already described by Lewis and Youle [36] we also observed comparable cytotoxicity in cells treated with high concentrations of intact or pre-reduced ricin. However, incubation with the selective TrxR inhibitor auranofin resulted in decreased cytotoxicity only in cells intoxicated by intact ricin, suggesting that the reduction of the disulfide holding together RTA and RTB subunits is needed within the cell. Clearly, the variable toxicity of ricin and/or RTA-ITs observed in different target cells could be only partly ascribed to the relative efficiency of the processes involving intracellular reduction/activation. Of course, differences in sensitivity to ricin in different cell lines could be due also to other processes (e.g. internalization, intracellular trafficking). With pre-reduced ricin, which bypasses the enzymatic reductive activation within the cell, the pattern of <sup>14</sup>C-leucine incorporation was U-937 > DU145 > Molt-3 > Jurkat without any significant difference between cells pre-incubated with auranofin and control without auranofin. However, ricin cytotoxicity is not completely prevented by incubating cells with auranofin and this may imply that additional mechanisms to those described here might function to reductively activate ricin/ITs and help deliver RTA in the cytosol of living cells. In fact auranofin can also induce the synthesis of some other protein such as heme oxygenase (a 34-kDa protein) and a 23-kDa protein with antioxidant activity in the cell exposed to oxidative stress [48]. Further, an example of cooperation between Hsp90 and TrxR in the cytosol entry of the catalytic subunit of DT was elegantly described recently by Ratts et al. [49].

Because reductive activation of ricin and of RTA-ITs takes place in compartmentalized environments it is likely that the cytosolic Trx and glutaredoxin systems participate only negligibly to this cell intoxication step. Instead, due to their intracellular distribution TrxR and PDI could be cooperatively involved in the process of intracellular

reductive activation of ricin and RTA-ITs. Indeed results of confocal microscopy confirmed that TrxR and PDI colocalize in a juxtannuclear region of the cell, possibly ER or related intracellular compartments (not shown).

In conclusion, our finding that TrxR exerts a fundamental role in ricin and RTA-ITs reduction/activation may open the way to strategies of modulation of the cytotoxic effects of these reagents, both in terms of negative (e.g. in case of ricin intoxication due to accidental or criminal occurrences) and positive (e.g. to enhance the cell-selective eradication of target cells by RTA-ITs) regulation.

## Acknowledgments

This work was partially supported by grants from Associazione Italiana per la Ricerca sul Cancro (AIRC) and Fondazione Cariverona, Bando 2001 “Ambiente e sviluppo sostenibile” to M.C.; and from University of L’Aquila, “Progetti di interesse di Ateneo 2001” to R.I.

## References

- [1] Fraser ME, Chernaia MM, Kozlov YV, James MN. Crystal structure of the holotoxin from *Shigella dysenteriae* at 2.5 Å resolution. *Nat Struct Biol* 1994;1:59–64.
- [2] Choe S, Bennett MJ, Fujii G, Curmi PM, Kantardjiev KA, Collier RJ, et al. The crystal structure of diphtheria toxin. *Nature* 1992;357:216–22.
- [3] Collier RJ, McKay DB. Crystallization of exotoxin A from *Pseudomonas aeruginosa*. *J Mol Biol* 1982;157:413–5.
- [4] Zhang RG, Scott DL, Westbrook ML, Nance S, Spangler BD, Shipley GG, et al. The three-dimensional crystal structure of cholera toxin. *J Mol Biol* 1995;251:563–73.
- [5] Montfort W, Villafranca JE, Monzingo AF, Ernst SR, Katzin B, Rutenber E, et al. The three-dimensional structure of ricin at 2.8 Å. *J Biol Chem* 1987;262:5398–403.
- [6] Ghetie V, Vitetta ES. Chemical construction of immunotoxins. *Mol Biotechnol* 2001;18:251–68.
- [7] Thrush GR, Lark LR, Clinchy BC, Vitetta ES. Immunotoxins: an update. *Annu Rev Immunol* 1996;14:49–71.
- [8] Falnes PO, Sandvig K. Penetration of protein toxins into cells. *Curr Opin Cell Biol* 2000;12:407–13.
- [9] Sandvig K, Grimmer S, Lauvrak SU, Torgersen ML, Skretting G, van Deurs B, et al. Pathways followed by ricin and Shiga toxin into cells. *Histochem Cell Biol* 2002;117:131–41.
- [10] Endo Y, Mitsui K, Motizuki M, Tsurugi K. The mechanism of action of ricin and related toxic lectins on eukaryotic ribosomes. The site and the characteristics of the modification in 28 S ribosomal RNA caused by the toxins. *J Biol Chem* 1987;262:5908–12.
- [11] Orlandi PA. Protein-disulfide isomerase-mediated reduction of the A subunit of cholera toxin in a human intestinal cell line. *J Biol Chem* 1997;272:4591–9.
- [12] Majoul I, Ferrari D, Soling HD. Reduction of protein disulfide bonds in an oxidizing environment. The disulfide bridge of cholera toxin A-subunit is reduced in the endoplasmic reticulum. *FEBS Lett* 1997;401:104–8.
- [13] Tsai B, Rodighiero C, Lencer WI, Rapoport TA. Protein disulfide isomerase acts as a redox-dependent chaperone to unfold cholera toxin. *Cell* 2001;104:937–48.
- [14] Tsai B, Ye Y, Rapoport TA. Retro-translocation of proteins from the endoplasmic reticulum into the cytosol. *Nat Rev Mol Cell Biol* 2002;3:246–55.
- [15] Arner ES, Holmgren A. Physiological functions of thioredoxin and thioredoxin reductase. *Eur J Biochem* 2000;267:6102–9.
- [16] Holmgren A. Antioxidant function of thioredoxin and glutaredoxin systems. *Antioxid Redox Signal* 2000;2:811–20.
- [17] Sahaf B, Soderberg A, Spyrou G, Barral AM, Pekkari K, Holmgren A, et al. Thioredoxin expression and localization in human cell lines: detection of full-length and truncated species. *Exp Cell Res* 1997;236:181–92.
- [18] Spyrou G, Enmark E, Miranda-Vizueta A, Gustafsson J. Cloning and expression of a novel mammalian thioredoxin. *J Biol Chem* 1997;272:2936–41.
- [19] Kurooka H, Kato K, Minoguchi S, Takahashi Y, Ikeda J, Habu S, et al. Cloning and characterization of the nucleoredoxin gene that encodes a novel nuclear protein related to thioredoxin. *Genomics* 1997;39:331–9.
- [20] Hirota K, Matsui M, Murata M, Takashima Y, Cheng FS, Itoh T, et al. Nucleoredoxin, glutaredoxin, and thioredoxin differentially regulate NF- $\kappa$ B, AP-1, and CREB activation in HEK293 cells. *Biochem Biophys Res Commun* 2000;274:177–82.
- [21] Hirota K, Nakamura H, Masutani H, Yodoi J. Thioredoxin superfamily and thioredoxin-inducing agents. *Ann NY Acad Sci* 2002;957:189–99.
- [22] Akagi S, Yamamoto A, Yoshimori T, Masaki R, Ogawa R, Tashiro Y. Localization of protein disulfide isomerase on plasma membranes of rat exocrine pancreatic cells. *J Histochem Cytochem* 1988;36:1069–74.
- [23] Pelham HR. The Florey Lecture, 1992. The secretion of proteins by cells. *Proc R Soc Lond B Biol Sci* 1992;250:1–10.
- [24] Tamura T, Stadtman TC. A new selenoprotein from human lung adenocarcinoma cells: purification, properties, and thioredoxin reductase activity. *Proc Natl Acad Sci USA* 1996;93:1006–11.
- [25] Sandalova T, Zhong L, Lindqvist Y, Holmgren A, Schneider G. Three-dimensional structure of a mammalian thioredoxin reductase: implications for mechanism and evolution of a selenocysteine-dependent enzyme. *Proc Natl Acad Sci USA* 2001;98:9533–8.
- [26] Lundstrom J, Holmgren A. Protein disulfide-isomerase is a substrate for thioredoxin reductase and has thioredoxin-like activity. *J Biol Chem* 1990;265:9114–20.
- [27] Frand AR, Kaiser CA. Ero1p oxidizes protein disulfide isomerase in a pathway for disulfide bond formation in the endoplasmic reticulum. *Mol Cell* 1999;4:469–77.
- [28] Fassio A, Sitia R. Formation, isomerisation and reduction of disulfide bonds during protein quality control in the endoplasmic reticulum. *Histochem Cell Biol* 2002;117:151–7.
- [29] Rozell B, Holmgren A, Hansson HA. Ultrastructural demonstration of thioredoxin and thioredoxin reductase in rat hepatocytes. *Eur J Cell Biol* 1988;46:470–7.
- [30] Soderberg A, Sahaf B, Rosen A. Thioredoxin reductase, a redox-active selenoprotein, is secreted by normal and neoplastic cells: presence in human plasma. *Cancer Res* 2000;60:2281–9.
- [31] Mustacich D, Powis G. Thioredoxin reductase. *Biochem J* 2000;346:1–8.
- [32] Sahaf B, Soderberg A, Ekerfelt C, Paulie S, Rosen A. Enzyme-linked immunospot assay for detection of thioredoxin and thioredoxin reductase secretion from cells. *Methods Enzymol* 2002;353:22–35.
- [33] Becker K, Gromer S, Schirmer RH, Muller S. Thioredoxin reductase as a pathophysiological factor and drug target. *Eur J Biochem* 2000;267:6118–25.
- [34] Soderberg A, Sahaf B, Holmgren A, Rosen A. Monoclonal antibodies to human thioredoxin reductase. *Biochem Biophys Res Commun* 1998;249:86–9.
- [35] Nicolson GL, Blaustein J. The interaction of *Ricinus communis* agglutinin with normal and tumor cell surfaces. *Biochim Biophys Acta* 1972;266:543–7.

- [36] Lewis MS, Youle RJ. Ricin subunit association. Thermodynamics and the role of the disulfide bond in toxicity. *J Biol Chem* 1986;261:11571–7.
- [37] Antin JH, Bierer BE, Smith BR, Ferrara J, Guinan EC, Sieff C, et al. Selective depletion of bone marrow T lymphocytes with anti-CD5 monoclonal antibodies: effective prophylaxis for graft-versus-host disease in patients with hematologic malignancies. *Blood* 1991;78:2139–49.
- [38] Magnusson CG, Bjornstedt M, Holmgren A. Human IgG is substrate for the thioredoxin system: differential cleavage pattern of interchain disulfide bridges in IgG subclasses. *Mol Immunol* 1997;34:709–17.
- [39] Gromer S, Arscott LD, Williams Jr CH, Schirmer RH, Becker K. Human placenta thioredoxin reductase. Isolation of the selenoenzyme, steady state kinetics, and inhibition by therapeutic gold compounds. *J Biol Chem* 1998;273:20096–101.
- [40] Holmgren A. Enzymatic reduction-oxidation of protein disulfides by thioredoxin. *Methods Enzymol* 1984;107:295–300.
- [41] Hwang C, Sinskey AJ, Lodish HF. Oxidized redox state of glutathione in the endoplasmic reticulum. *Science* 1992;257:1496–502.
- [42] Barbieri L, Battelli MG, Stirpe F. Reduction of ricin and other plant toxins by thiol:protein disulfide oxidoreductases. *Arch Biochem Biophys* 1982;216:380–3.
- [43] Jansen FK, Blythman HE, Carriere D, Casellas P, Gros O, Gros P, et al. Immunotoxins: hybrid molecules combining high specificity and potent cytotoxicity. *Immunol Rev* 1982;62:185–216.
- [44] Gilbert HF. Molecular and cellular aspects of thiol-disulfide exchange. *Adv Enzymol Relat Areas Mol Biol* 1990;63:69–172.
- [45] Tortorella D, Story CM, Huppa JB, Wiertz EJ, Jones TR, Bacik I, et al. Dislocation of type I membrane proteins from the ER to the cytosol is sensitive to changes in redox potential. *J Cell Biol* 1998;142:365–76.
- [46] Matsuo Y, Akiyama N, Nakamura H, Yodoi J, Noda M, Kizaka-Kondoh S. Identification of a novel thioredoxin-related transmembrane protein. *J Biol Chem* 2001;276:10032–8.
- [47] Aslund F, Berndt KD, Holmgren A. Redox potentials of glutaredoxins and other thiol-disulfide oxidoreductases of the thioredoxin superfamily determined by direct protein-protein redox equilibria. *J Biol Chem* 1997;272:30780–6.
- [48] Sato H, Yamaguchi M, Shibasaki T, Ishii T, Bannai S. Induction of stress proteins in mouse peritoneal macrophages by the antireumatic agents gold sodium thiomalate and auranofin. *Biochem Pharmacol* 1995;49:1453–7.
- [49] Ratts R, Zeng H, Berg EA, Blue C, McComb ME, Costello CE, et al. The cytosolic entry of diphtheria toxin catalytic domain requires a host cell cytosolic translocation factor complex. *J Cell Biol* 2003;160:1139–50.